The 2010 IEEE/RSJ International Conference on
Intelligent Robots and Systems
October 18-22, 2010, Taipei, Taiwan

Traction Force Characterization of Human Bipedal Motion

Andrew Vogt, Lucas Lincoln, Stacy J. Morris Bamberg, *Member, IEEE,* and Mark Minor, *Member, IEEE*

***Abstract*— Traction estimation and control, common in the automotive industry, have yet to be extended to human bipedal motion. This paper presents a novel metric for slip and traction optimization using the partial derivative of a traction force estimate to slip velocity. The metric is verified computationally using an existing dynamic mode and experimentally using a multi-camera motion capture system.**

I. Introduction

Slip is a difficult uncertainty which complicates effective operation of many dynamic systems. Slippery surfaces are found in 66% of fall-related hip fractures [1]. Realizing issues caused by slip, the automotive industry has made strides to both model and control slip and traction. Slip can be visualized as the relative velocity of the contact point between two surfaces. Traction, on the other hand, is the force between the two surfaces caused by slip. Both anti-lock braking systems (ABS) and traction control systems (TCS) modulate slip and attempt to control traction forces, with the goal of improving driver safety.

Although these systems work well for an average driver, they are incapable of maximizing traction forces. Experienced drivers, similar to athletes, have proprioception acutely attuned to their vehicular-terrain interaction; this provides an ability to modulate slip thereby improving traction forces beyond the capability of typical ABS or TCS systems. This paper illustrates that techniques to improve traction force by modulating slip can be readily extended to human bipedal motion. Important applications include rehabilitation, humanoid and bio-inspired robotics, and smart prosthetics.

Aside from maximizing traction forces, a valuable side-effect of these techniques is they are attuned to human proprioception. This could help individuals gain proprioceptive abilities similar to athletes. Specifically, this benefits individuals suffering from depleted tactile feedback. In addition, this research can help study why falls occur in patients with limited motor skills; this includes the elderly and Parkinson's disease patients.

The main objectives of this paper are to identify a human slip metric and illustrate the potential to maximize human traction force. The first critical step in this process is identifying a traction model.

The automotive industry bases many traction controllers on the causal relationship between wheel slip (λ) and tyre traction coefficient (μ), as illustrated for many surfaces in Fig. 1. λ is a non dimensional unit (further explained on the next page) where λ=0 and λ=1 mean no slip and full slip are occurring, respectively; μ is the standard Coulomb friction relationship. We hypothesize that a human exhibits a similar causal relationship between slip and traction force.

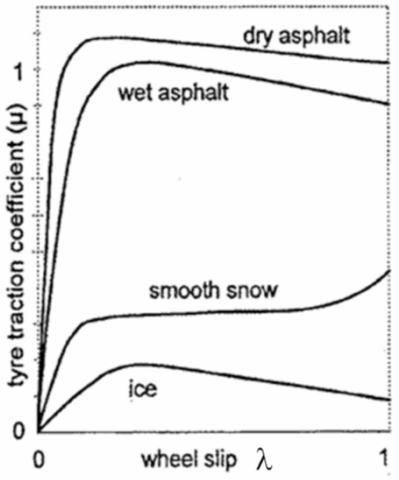

Fig. 1: Slip curves for typical surfaces [2, 3].

For most surfaces, the slip-traction curve (also called the 'slip curve' for simplicity) has the same characteristics: increasing λ from 0 causes μ to increase to a local maximum, where continuing to increase λ causes μ to decrease.

Problematically, the slip curve is highly variable and must be determined empirically for any change in surface conditions. Although we cannot determine all parameters of the curve with accuracy, this paper shows how we can identify the critical parameters needed for human traction control.

The rest of this paper is organized as follows: Section II contains pertinent background information illustrating the contributive nature of our research, section III explains how we can maximize traction force online, section IV presents results, section V discusses significant successful issues, section VI explores future work, and section VII reiterates this paper's important points and presents final concluding remarks.

II. Background

Based on our prior work [4], a standard slip curve is commonly used to determine the relationship between wheel

Manuscript received March 11, 2010. This work was supported in part by NSF Grant No DGE-0654414

Andrew Vogt is with the Department of Mechanical Engineering, University of Utah, Salt Lake City, UT 84112 USA. (phone: 801-587-9018, e-mail: vogt@eng.utah.edu).

Lucas Lincoln is with the Department of Mechanical Engineering, University of Utah, Salt Lake City, UT 84112 USA. (phone: 801-587-9018, e-mail: lucas.lincoln@utah.edu).

Stacy Bamberg is with the Department of Mechanical Engineering, University of Utah, Salt Lake City, UT 84112 USA. (phone: 801-587-9018, e-mail: sjm.bamberg@utah.edu).

Mark Minor is with the Department of Mechanical Engineering, University of Utah, Salt Lake City, UT 84112 USA. (e-mail: minor@mech.utah.edu).

slip and traction force. [4] was inspired by the European Delft-Volvo collaboration, led by Pacejka in the early 90's, which established the physics-inspired "magic tyre formula" [5]. The advantages of this model are its high adaptability to varying terrain. While suited for hard surfaces, such as pavement [6], experimental data shows applicability of these fundamental models to other surfaces such as sandy loam [7] as well as snow and ice [8]. Typical analytical models, on the other hand, are often so intensive that they are used offline in Finite Element Methods (FEM) or vehicle dynamics analysis. Striving for simplicity and computational speed, some researchers rely upon empirical models for traction characterization, but include specific analytic terms to better improve accuracy [9-11]

Perhaps the greatest application of this research is helping those with limited tactile feedback. Guillian Barré patients suffer from a acute peripheral neuropathy hindering their ability to sense or actuating their peripherals [12]. Research has already shown the benefits of improving prosthetics with pressure sensing devices [13], but our goal is to provide patients more complete sensing capabilities by giving them a sense of traction.

At slow gait speeds, self-selected by older adults, falls caused by slips typically impact the hip area, risking fracture of the femur [14]. Dynamic posture depends on proprioceptive, vestibular, and visual sensory inputs, and is affected by perturbations [15] and shaped by an internal representation of body dynamics [16]. Although the coefficient of friction between the foot and walking surface is important, foot kinematics of the foot at heel strike are also critical [17]. Our traction control research would allow us to further evaluate impacts on foot traction in human stability.

III. Methods

We develop human slip principles analogous to established wheeled slip principles as follows:

A. Wheel-Based Definition of Slip

The methods developed by our research are aimed at identifying critical parameters of the slip curve. Parameters defining the point of maximum force (μ_{max}) and corresponding slip (λ_{max}) are arguably the most important because they segregate the region of stable monotonically increasing traction force given increasing slip (when $0 < \lambda < \lambda_{max}$) and the region of unstable monotonically decreasing traction force given increasing slip (when $\lambda_{max} < \lambda < 1$).

As prior stated, using the slip curve to develop traction control has primarily been considered for wheeled vehicles. To understand how slip is defined for human motion then it is useful to consider first the definition for wheeled vehicles. Slip for wheeled vehicles is simply a comparison of translational to rotational speed:

$$\lambda = 1 - \frac{v}{\omega \cdot r_w} = \frac{\omega - v/r_w}{\omega}, \text{ where } 0 < \lambda < 1. \quad (1)$$

In (1), ω is angular speed, v is translational speed, and r_w is the radius of the wheel. The problem, as demonstrated by our prior research [4], is that mobile robots have ill-posed λ because they travel at slow speeds. This happens because as angular velocity approaches zero, λ approaches a singularity. We therefore define a new metric, slip velocity (α), such that

$$\alpha = \omega - v/r_w, \quad (2)$$

which eliminates the denominator of (1).

A *wheel with no slip* exhibits $\alpha = 0$, therefore

$$\omega_{NS} = v/r_w, \quad (3)$$

where ω_{NS} is the no-slip angular speed (i.e. angular speed *only* contributing to forward motion).

In the event of *pure wheel slip*

$$v = 0 \text{ and } \omega = \omega_s \Rightarrow \alpha = \omega_s \quad (4)$$

where ω_S is the amount of angular speed that does not contribute to translational speed. In pure slip, therefore, the slip velocity is exactly equal to ω_S .

In (2), ω can be replaced with the addition of ω_S and ω_{NS} as follows

$$\alpha = \omega_{NS} + \omega_S - v/r_w. \quad (5)$$

Then, (3) can be substituted into (5) which results in

$$\alpha = \omega_s = v_s / r_w \quad (6)$$

v_S is the tangential velocity contributing *only to* wheel slip and has *absolutely no* contribution to translational motion. We can re-define translational slip velocity as

$$\alpha_{TRANS} = v_s = \alpha r_w \quad (7)$$

Because r_W does not change, α and α_{TRANS} change linearly with respect to each other. The greatest result of (7) is a slip velocity metric independent of ω, linearly related to α, and most importantly able to be applied directly to human motion.

B. Human-Based Translation Slip Velocity

Slip for bipedal motion could be defined very similarly to (6) where r_W is approximately equal to the distance between the ankle and hip (i.e. the distance to the center of rotation). Nevertheless it remains desirable to have a metric independent of r_W because gait could significantly alter r_W deeming (6) unreliable. (7)'s independence of r_W, on the other hand, makes it an ideal slip metric.

Though α_{TRANS} is mathematically different than λ,, our experiments show that the general shape of the human-based slip curve remains intact in comparison to Fig. 1. Fig. 2 shows plots the slip curves (shear force v. α_{TRANS}) of both heel-contact (HC) and toe-release (TR) data for normal and induced slip gaits. Their similarity to the automotive industry's λ v. μ curves (Fig. 1) offer justification in applying wheel vehicle traction principles to bipedal motion.

In addition, α is more tractable than λ because it compares ω and v on range from 0 to ω rather than a range restricted between 0 and 1. This is a particularly nice extension for humans because our abundance of senses make it difficult to

purely isolate relative slip. It is shown in subsection *C* that is just as usable as for determining critical slip curve parameters.

C. Critical Slip Curve Parameters

Recall, as discussed previously, there are two distinct regions on the slip curve: One where traction force is monotonically increasing; and one where it is decreasing. We can identify our location on the slip curve by its slope, defined as: $\beta = \partial\mu / \partial\lambda$ In terms of slope and stability,

$$\begin{aligned} &\beta > 0 \text{ (stable slip)} \\ &\beta = 0 \text{ (marginally stable slip)} \\ &\beta < 0 \text{ (unstable slip)} \end{aligned} \tag{8}$$

Likewise, using our new slip metric α, we can define a analogous slope:

$$\hat{\beta} = \frac{\partial\tau(t)}{\partial\alpha(t)} = \frac{\partial\tau(t)}{\partial t}\left(\frac{\partial\alpha(t)}{\partial t}\right)^{-1} \tag{9}$$

effectively replacing β for characterizing stability. In (9), τ represents an estimation of traction force, which can be determined by force sensors or observer systems.

If we assume the radius of rotation of the leg is constant, then $\partial\alpha_{TRANS} = \partial\alpha$. This affords the benefit of using a wheeled model (developed in [3]) to verify $\hat{\beta}$ for both wheeled mobile robots and human motion.

First, typical traction curves are generated (Fig. 3) for smooth, medium, and rough surfaces. (9) is validated by linearly increasing λ in a single wheel dynamic simulation. The resulting estimates of ω and $\dot{\omega}$ are used to determine α, using the slip velocity estimator in [4], and $\hat{\beta}$, using (9). shows the simulation results of the actual slope, β, compared to the estimated slope $\hat{\beta}$. Although the magnitudes do not coincide, they have the same sign and cross zero at the exact same time. In other words:

$$\begin{aligned} &\hat{\beta} > 0 \Rightarrow \beta > 0 \text{ (stable)} \\ &\hat{\beta} = 0 \Rightarrow \beta = 0 \text{ (marginally stable)} \\ &\hat{\beta} < 0 \Rightarrow \beta < 0 \text{ (unstable)} \end{aligned} \tag{10}$$

The critical comparison is whether both β and $\hat{\beta}$ cross zero simultaneously which indicates that either one can be used to indicate system stability. This simultaneous switching characteristic, between β and $\hat{\beta}$, are also observed while simulating more complicated time varying slip (including sinusoids or the addition of white noise). The increasing difference between β and $\hat{\beta}$ can be attributed to a greater amount of ground friction causing greater modeling uncertainly.

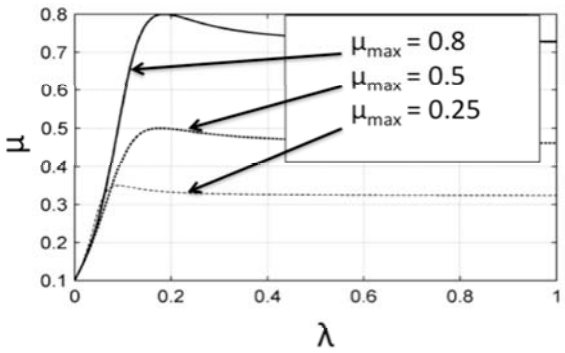

Fig. 3. Traction curves generated for validation.

Recall it is necessary to know the slope ($\hat{\beta} = \partial\tau / \partial\alpha$) opposed to *only* $\partial\tau(t)$ in order to identify the required $\pm\alpha$ modulation to approach the traction maximum.

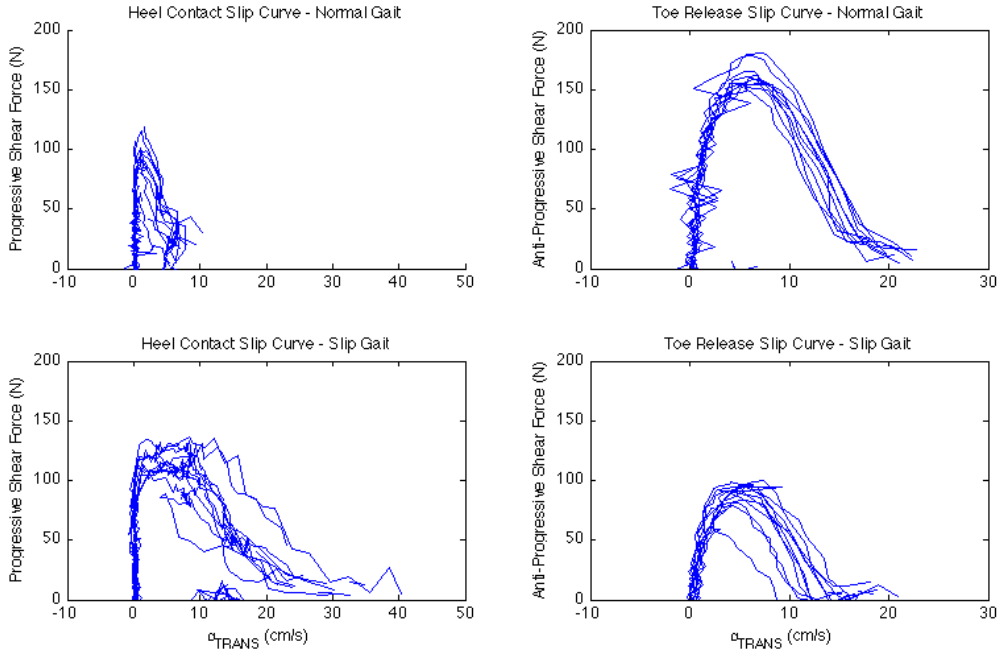

Fig. 2: α-τ slip curves generated for human slip. which correlate well to Fig. 1.

IV. Experimental Procedures

To experimentally verify $\hat{\beta}$, we used a motion analysis lab. The workspace of this lab, shown in the subfigures of Fig. 5, consisted of a passive-marker stereographic camera system to capture kinematic motion (primarily v_{TRANS}); and a three-axis force plate covered with a surface affording slip to capture traction forces. The

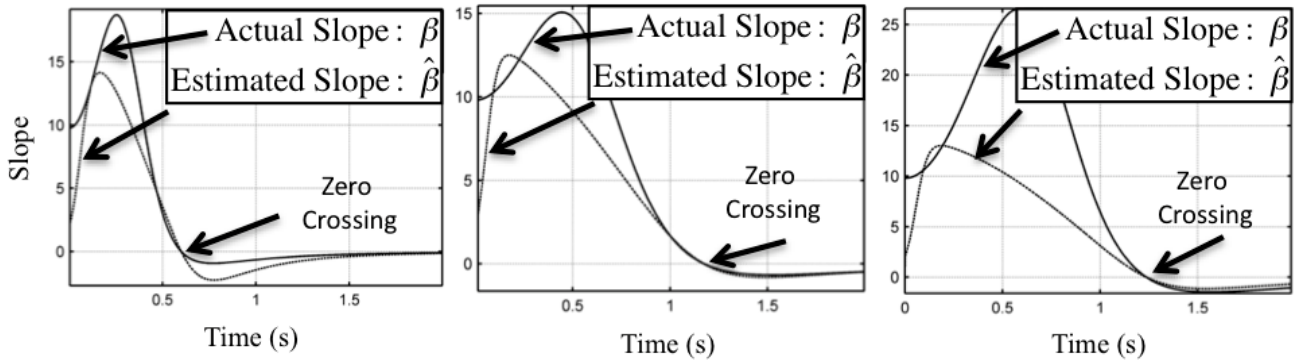

(a) $\mu_{\max} = 0.25$ (b) $\mu_{\max} = 0.50$ (c) $\mu_{\max} = 0.80$

Fig. 4. Traction curve slopes.

sampling frequencies, which are sufficient for capturing human motion (typically under 30 Hz), are 1000 Hz for both the kinematic motion capture cameras and the three-axis force plate. The slip surface consisted of a sheet of 'painter's plastic' secured to the floor surrounding the force plate and an additional loose sheet of plastic atop used to produce a shearing layer. Although experiments conducted in this paper use idealized velocity measurements, with a Vicon motion capture system, other avenues of our research have demonstrated that MEMS inertial sensors are capable of identifying the onset on slip [18].

The test gait of interest was a right foot slip and step-through, because it explored shear in both directions as well as a point where $\alpha_{TRANS} \to 0$. This procedure is illustrated in Fig. 5:

1. The subject approached the slip surface, and on heel strike begins to slip.
2. During slip, the subject continues his stride, causing his toes to contract the ground.
3. The subject regains balance by swinging his left foot forward, and in the process puts significantly more weight on the ball of his right (slipping) foot.
4. The subject removes his toes from ground.

V. Results

Fig. 6 shows the corresponding data for the procedure shown in Fig. 5. The left subfigures are the x and z positions, respectively. For this test, the zone between ~40-100 centiseconds is analyzed because this is the period in which the subject contacts the force plate. Fig. 7 presents an

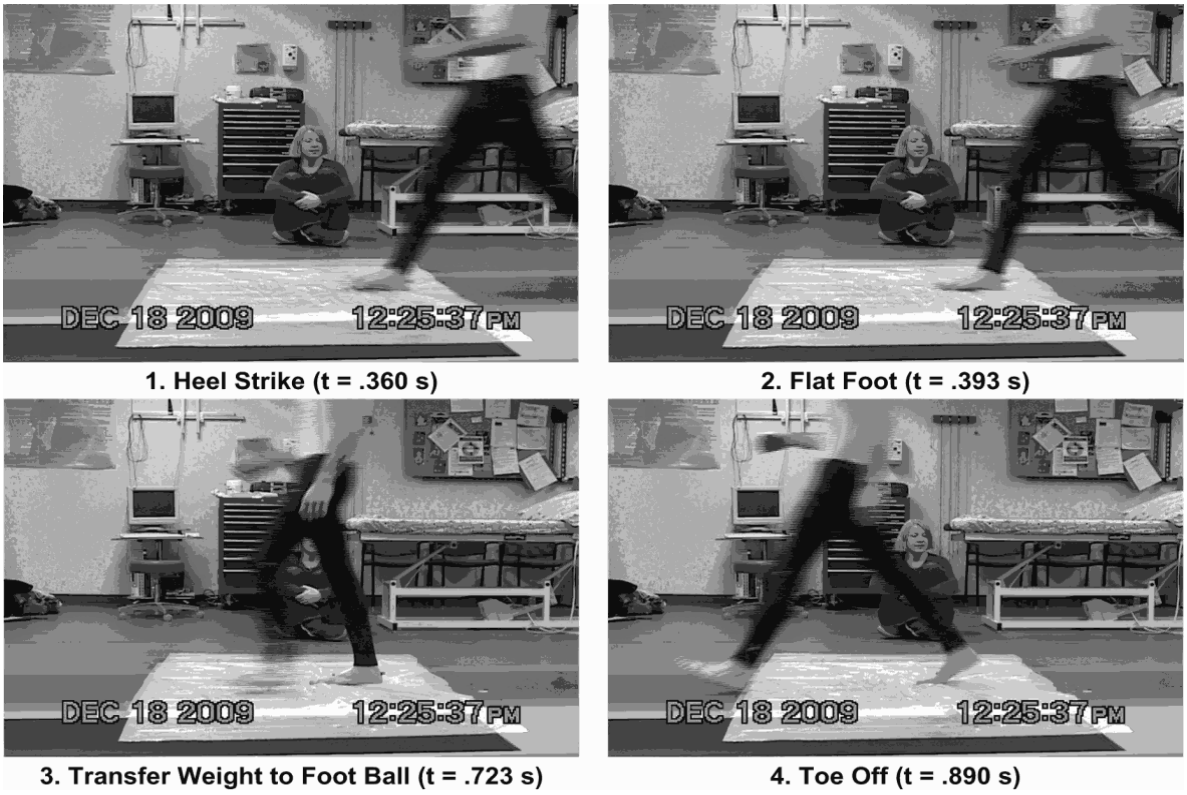

Fig. 5: Experimental Procedure. The walking subject steps on a 'slick surface' on top of a force plate with his right foot while a passive-marker stereographic camera system captures his motion. The corresponding data for this figure can is found in Fig. 6.

additional data set, using the same gait; although (instead of painter's plastic) glossy paper was used as the shearing layer. Both Fig. 6 and Fig. 7 are based on ankle velocity measurements. Fig. 8 is presented as a comparison using velocity of both ankle versus toe.

VI. Discussion and Future Work

All results show a good response to our predictions: Namely, $\hat{\beta}$ corresponds to traction force change. There are two discussion points of greatest interest: First, there must be a reasonable amount of slip to determine whether traction force is increasing or decreasing. Second, modeling and perhaps data fusion are critical for advancing this research.

Regarding the first discussion point, consider the heel contact (HC) and toe release (TR) regions of slip in Fig. 6 and Fig. 7 (HC: 32cs-53cs and 97cs-113cs, respectively; TR: 90cs-98cs and 113cs-117cs, respectively). These regions accurately predict our hypotheis of simultaneously changing signs of $\hat{\beta}$ and shear force. Notably, the relationship holds true for positive and negative axial shear, both of which exist in typical human gaits.

These common regions share high slip velocities. The other regions have low slip velocities and little correspondence between $\hat{\beta}$ and shear force as well as the occurrence of singularities. So, we hypothesize that as $\partial\alpha_{TRANS} \to 0$ reliability between $\hat{\beta}$ and shear force decreases.

The HC region has a larger period of correct correspondence between $\hat{\beta}$ and shear force than the TR region. We expect this is because Fig. 6 and Fig. 7 are developed from ankle velocities, which worked well for the HC region but not for the TR region. For the TR region, the heel begins to pick up and the foot deflects, relative to its ground contact at the toe, thus no longer providing an accurate representation of slip velocity. Additional data, seen in Fig. 8, supports this explanation as the correlation between $\hat{\beta}_{ankle}$ and shear force is better for the HC region, whereas the correlation between $\hat{\beta}_{toe}$ and shear force is better for the TR region.

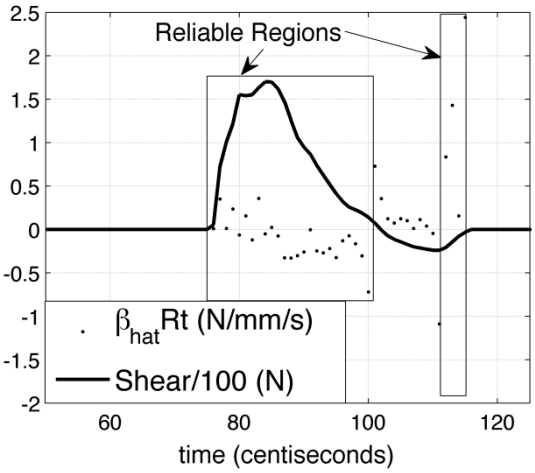

Fig. 7: Glossy paper slip data showing the difference between $\hat{\beta}$ and shear force.

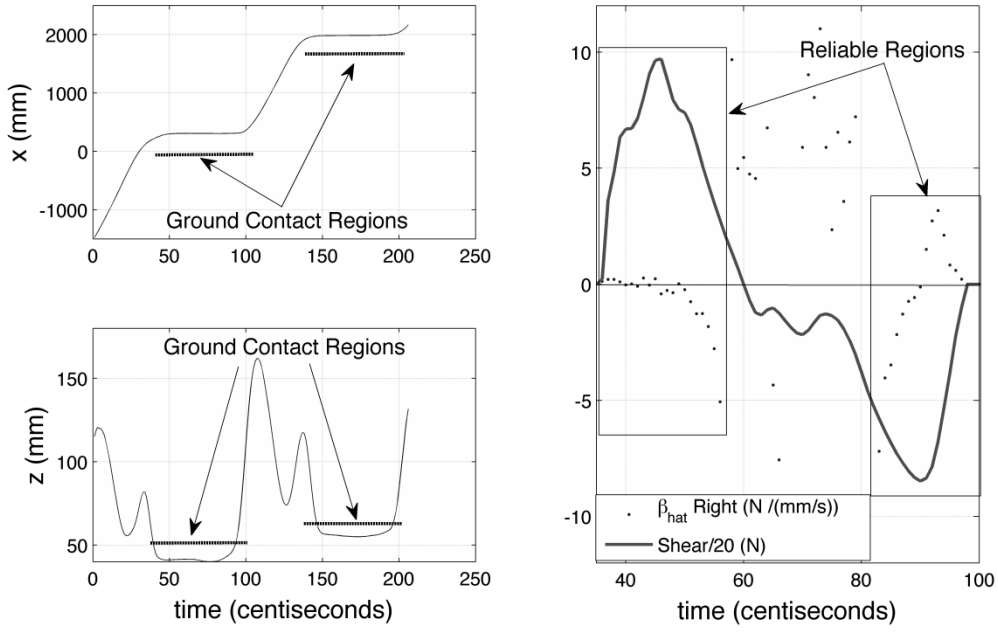

Fig. 6: Slip trial corresponding to Fig. 5. The left subfigures are the x and z ankle (only) positions, respectively; these are useful for knowing when the foot stops moving (x) and when it hits the ground (z). The period between ~40-100 centiseconds is in contact with the force plate. The right subfigure compares $\hat{\beta}$ to shear force.

Regarding further application of this research, modeling is critical in order to compute $\hat{\beta}$ online. A human dynamic model will be required to predict traction force in the absence of force plate readings. In addition, we discovered that the accuracy of beta depends where on the foot slip velocity is considered. In most cases, this is a point which is in contact with the ground. Our previously developed foot-bed sensors [19] are ideal for his purpose. Our future work will be in developing a dynamic gait model and wearable sensor arrangement capable of predicting traction force and accurately measuring slip velocity.

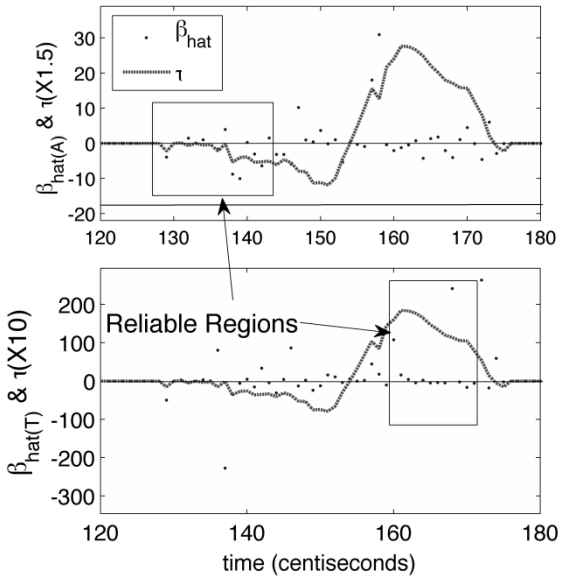

Fig. 8: Addition data comparing $\hat{\beta}$ to shear force for the ankle (top subfigure) and toe (bottom subfigure).

VII. Conclusion

This paper explored the analogs between wheel and human traction control principles. We developed a slip metric capable of identifying required actions to maximize traction force, based on the popular slip-traction curve and its slope. This research is an ideal proof of concept for future work involving wearable inertial measurement units, foot pressure sensors, and smart prosthetic design.

Acknowledgements

We would like to thank Bruce MacWilliams of Shiner's Childrens Hospital in Salt Lake City, Utah for access to motion capture facilities.

References

1. Norton, R., Campbell, J., Lee-Joe, T., Robinson, E. and Butler, M., *Circumstances of falls resulting in hip fractures among older people.* Journal of the American Geriatrics Society, 1997. 45(9): p. 5.
2. van der Burg, J. and P. Blazevic. *Anti-lock braking and traction control concept for all-terrain robotic vehicles*. in *Proceedings of the 1997 IEEE International Conference on Robotics and Automation, ICRA. Part 2 (of 4), Apr 20-25 1997*. 1997. Albuquerque, NM, USA: IEEE, Piscataway, NJ, USA.
3. Colli, V., G. Tomassi, and M. Scarano, *"Single Wheel" longitudinal traction control for electric vehicles.* IEEE Transactions on Power Electronics, 2006. 21(3): p. 799-808.
4. Terry, J.D. and M.A. Minor. *Traction estimation and control for mobile robots using the wheel slip velocity*. 2008. Piscataway, NJ, USA: IEEE.
5. Pacejka, H.B. and E. Bakker, *Magic formula tyre model*, in *Vehicle System Dynamics Proceedings of the 1st International Colloquium on Tyre Models of Vehicle Dynamics Analysis*. 1993, Swet. p. 1-18.
6. Fancher, P.S., Jr. and Z. Bareket, *Including roadway and tread factors in a semi-empirical model of truck tyres.* Vehicle System Dynamics, 1993. 21(SUPPL): p. 92-107.
7. Vechinski, C.R., C.E. Johnson, and R.L. Raper, *Evaluation of an empirical traction equation for forestry tires.* Journal of Terramechanics, 1998. 35(1): p. 55-67.
8. Shoop, S., et al., *Winter traction testing.* Automotive Engineering (Warrendale, Pennsylvania), 1994. 102(1): p. 75-78.
9. Sharp, R.S. and M. Bettella, *On the construction of a general numerical tyre shear force model from limited data.* Proceedings of the Institution of Mechanical Engineers, Part D: Journal of Automobile Engineering, 2003. 217(3): p. 165-172.
10. Gafvert, M. and J. Svendenius, *A novel semi-empirical tyre model for combined slips.* Vehicle System Dynamics, 2005. 43(5): p. 351-84.
11. Ortiz, A., et al., *Analysis and evaluation of a tyre model through test data obtained using the IMMa tyre test bench.* Vehicle System Dynamics, 2005. 43(SUPPL): p. 241-252.
12. Hughes, R.A., Comblath, D.R., *Guillain-Barre syndrome.* The Lancet, 2005. 336(9497): p. 1653-1666.
13. Chizeck, H.J., P.M. Selwan, and F.L. Merat. *A foot pressure sensor for use in lower extremity neuroprosthetic development*. 1985. Washington, DC, USA: Rehabilitation Eng. Soc. North America.
14. Smeesters, C., W.C. Hayes, and T.A. McMahon, *Disturbance type and gait speed affect fall direction and impact location.* Journal of Biomechanics, 2001. 34(3): p. 309-317.
15. Johansson, R. and M. Magnusson, *Human postural dynamics.* Crit Rev Biomed Eng, 1991. 18(6): p. 413-37.
16. van der Kooij, H., et al., *An adaptive model of sensory integration in a dynamic environment applied to human stance control.* Biol Cybern, 2001. 84(2): p. 103-15.
17. Cham, R. and M.S. Redfern, *Lower extremity corrective reactions to slip events.* Journal of Biomechanics, 2001. 34(11): p. 1439-45.
18. Lincoln, L., Bamberg, S.M., *Insole Sensor System for Real-Time Detection of Biped Slip*, in *2010 IEEE Engineering in Medicine and Biology Society*. 2010, IEEE: Buenos Aires, Argentina.
19. Bamberg, S., et al., *Gait analysis using a shoe-integrated wireless sensor system.* IEEE Transactions on Information Technology in Biomedicine, 2008. 12(4): p. 413-23.